

The Intermediate Prototype Development of the Compressor Drive for a Fuel Cell Power System

K.O. Boinov, E.A. Lomonova, A.J.A. Vandenput

Technical University of Eindhoven
Department of Electrical Engineering
P.O.Box 513 - 5600 MB
Eindhoven, The Netherlands
Tel: +31 40 2473574/ Fax: +31 40 2434364
e-mail: k.boinov@tue.nl

Acknowledgements

The authors thank Dr. J.L. Duarte, Dr. Ir. H.C. de Lange, Dr. Ir. L.J.J. Offringa, Ir. J.L.F. van der Veen (TU Eindhoven) and Elektromotorenfabriek Nijmegen BV for valuable discussions and assistance.

Keywords

Control, Efficiency, Energy system management, Fuel Cell Systems, Induction motors, Variable speed drives.

Abstract

The paper summarises several initial steps of configuration and analysis of the system with an air compressor and an electrical drive for the application in a fuel cell (FC) power system (power level is 250 kW). The preliminary FC system configuration procedure with respect to the compression system is reviewed. The dynamic mathematical model of the centrifugal compressor is presented. The preliminary selection of the high-speed induction motor and its parametric optimisation are done by means of design assistant program RMxpert (Ansoft Co.). The performance characteristics of the induction motor are obtained and evaluated for the different compressor system operation points. The transient analysis of the motor is accomplished in the finite element package Maxwell 2D (Ansoft Co). All predictions are validated against the benchmark motor.

1. Introduction

The fuel cell power generation system is regarded as one of the perspective energy supply solutions for multiple applications. In particular, proton exchange membrane fuel cells (PEMFC) are becoming an alternative energy source for vehicular, stationary (distributed generation) and auxiliary power applications.

In addition to the primary system components (FC stack, electronic power conditioner, heat exchanger) which are employed in power production and distribution, there are auxiliary components (e.g. air compressor, cooling blower with the electrical drives, etc.) required to supply reactant gasses to the stack and maintain the necessary operation conditions (pressure, temperature, humidity, etc) for the power system.

The FC systems can be subdivided into pressurized and ambient pressure ones. Analysing the published studies dedicated to FC air management systems' design and their operation profiles [1] – [5], the relative advantages and disadvantages of pressurized and non-pressurized FC can be summarized (Table I). The

main disadvantages in the pressurized system arise due to the usage of an air compressor instead of a blower. The existing problems in pressurized systems encourage the development of an efficient, reliable and low cost equipment for pressurization, fitted for the mentioned power system and its operation regimes.

The current paper describes several aspects of the FC air system design. The optimum between the system energy efficiency and performance is accepted as an initial point for the primary choice of the compressor system components and their further optimisation and control development. The modern centrifugal compressor equipped with a high speed induction motor drive is considered a major candidate for the FC application.

Table I: Relative pros and cons of pressurized and non-pressurized FC system

	Pros	Cons
Pressurized FC system	Higher power density Higher value of current Rapid response Higher FC stack efficiency	Higher compressor power losses Noisy operation Increased system complexity
Ambient pressure FC system	Lower blower losses Salient operation Reduced system complexity	Lower power density Lower value of load current Slower response Lower FC stack efficiency

2. System configuration development procedure

2.1. FC system configuration with respect to pressurization

The following procedure for the FC system configuration can be proposed (Fig. 1).

First, the initial requirements for the whole fuel cell power system such as efficiency and response time are formulated. Further, certain boundaries (maximum current level, size, cost, etc) are established. If the designed FC satisfies the mentioned demands, the pressurisation is not necessary. In practice, low power systems (1-10 kW) are designed for ambient pressure operation.

However, for higher power level applications (50-250 kW) with more strict requirements for the size or power density and dynamic responses, pressurisation is desired. Thus, the appropriate compression system has to be installed.

The simplified compression system with a constant speed compressor and electrical drive can be used. In this case, all system components operate at the rated regime (or in mode "ON/OFF"). In practice, such systems have to be equipped by a large buffer battery pack. The use of them is undesired due to the known weak points of batteries.

One of the possible improvements of the pressurized system performance is related to the so-called load following operation of the compressor. It means, that the compressor speed, pressure, air mass flow are varied proportionally to the FC electrical load level. This approach leads to the improved system efficiency, due to the adjustable power consumption by the compressor. However, in a system with intensive load duty cycle, a system response delay can be caused by the limited acceleration of the compressor.

Finally, an alternative way of the FC compressor operation profile can be proposed, where the air mass flow and pressure are independently controlled. Such a method allows reduction of compressor energy consumption, while keeping the fuel cells dynamic performance at a high level.

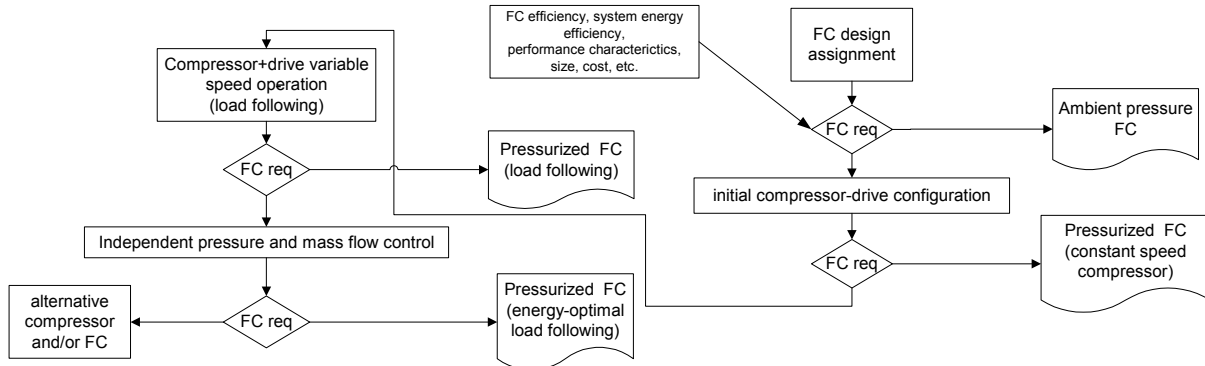


Fig. 1: FC system development with respect to the compression system and electrical drive

The last method is not widely used in compression systems due to the limited operation area of centrifugal compressors. The novel methods of centrifugal compressor stabilisation (surge control) can allow an operation at the point with a reduced level of mass flow and lower energy consumption [6].

2.2. Centrifugal compressor model

The current study deals with a compressor of centrifugal type, which is commonly used in different air pumping applications and has appropriate characteristics to be used in a fuel cell system. The pressure is created due to the conversion of the kinetic energy of the gas. Centrifugal compressors have a low cost, they are well developed, and their efficiency is comparable with that of any other type [2].

The compression system model based on the Greitzer model with lumped parameters (Fig. 2) consists of the centrifugal compressor, compressor duct, plenum volume and a throttle [6]. The plenum is defined as the equivalent air volume within the FC stack.

The dynamic model is described by equations (1) – (3):

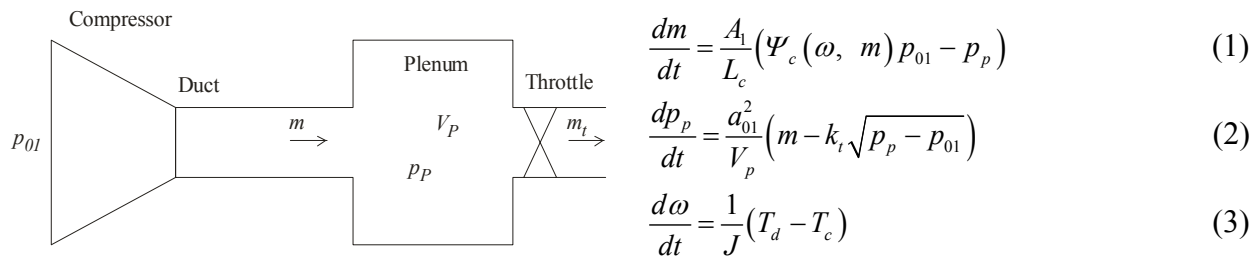


Fig. 2: The compressor, plenum, throttle system

where

Ψ_c – compressor characteristics, m – compressor mass flow (kg/s), a_{01} – inlet stagnation sonic velocity (m/s), L_c – length of compressor and duct (m), A_l – area of impeller eye (m²), J – spool moment of inertia (kgm²), ω – compressor angular speed (rad/s), p_{01} – ambient pressure (Pa), p_p – plenum pressure (Pa), V_p –

plenum volume (m^3), T_d – drive torque (Nm), T_c – compressor torque (Nm), k_t – throttle gain. Compressor torque is defined as: $T_c = m\sigma\omega r_2^2$ where σ – slip factor, r_2 – impeller radius (m).

The operation area of centrifugal compressors is limited by the “surge” line which defines the stability margins in the compressor map. The surge is an unstable operation mode of centrifugal compressors which occurs when the operating point of the compressor is in the vicinity of the surge line. The surge has been a major problem for designers and users since the invention of the turbo compressor. The surge phenomenon consists of oscillations of the mass flow, pressure and rotational speed of the compressor. Its occurrence is highly undesired and can cause severe damage to the machine.

Traditionally, the surge has been avoided using the “surge avoidance” schemes. The surge avoidance method uses various techniques to keep the operating point of the compressor away from the surge line. This method works properly, as has been proved by numerous installations. However, due to the presence of the surge margin, the method restricts the operating range of the machine.

Active surge control is fundamentally different from surge avoidance as unstable equilibria are sought to be stabilized instead of avoided. The motivation behind this is to overcome some of the limitations of surge avoidance. One of the active surge control methods employs the so-called close coupled valve (CCV), installed in series with the compressor [6]. The occurring effect is equivalent to introducing additional friction to the air flow which produces a stabilizing effect. The result of this is that the surge line is shifted to the left, and the area of stable compressor operation is expanded.

A distinctive active surge control method by means of an electrical drive powering the compressor is proposed in [7]. The method is based on the torque/speed control of the electrical drive which powers the compressor. In this approach, the electrical drive itself is used for surge control, thus eliminating the need for additional actuators. The compressor can operate at low mass flow without surge providing the extension of the compressor operation area. The rotational speed or drive torque can be chosen as a control variable, depending on the applied control scheme. The stability is proven with the use of the Lyapunov method [7]. The following simulation results (Fig. 3) of the model (1) – (3) represent the compressor operation in the stable area, surge mode and with surge control.

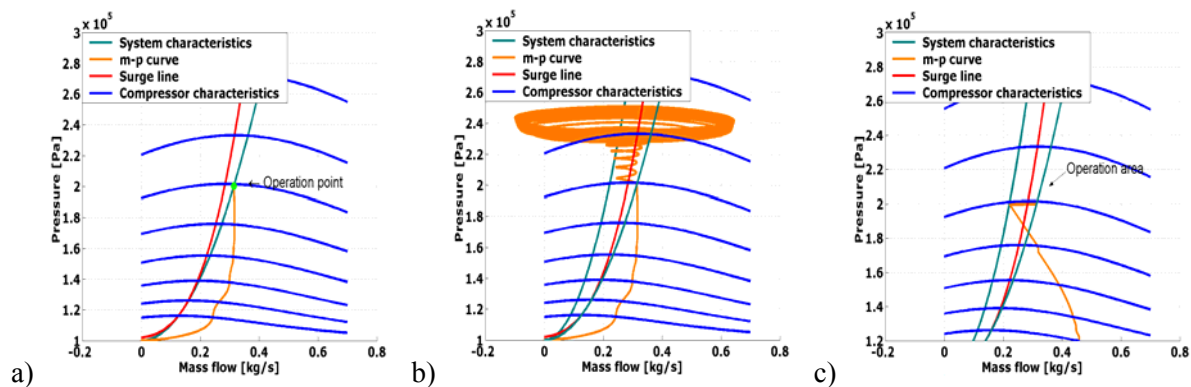


Fig. 3: Centrifugal compressor simulation results; a) Stable operation area, b) Surge, c) Surge control

3. Development procedure of the electrical drive for the compressor

High speed AC-drives employing induction motors with static converters are serious candidates for the discussed type of applications. Global competition makes a comprehensive theoretical design analysis mandatory in order to accurately predict the drive system performance as well as to exploit the potential for optimization in a view of short industrial development cycles. The following flowchart (Fig. 4) demonstrates the general development, synthesis and optimisation strategy for the FC compressor drive with an induction motor.

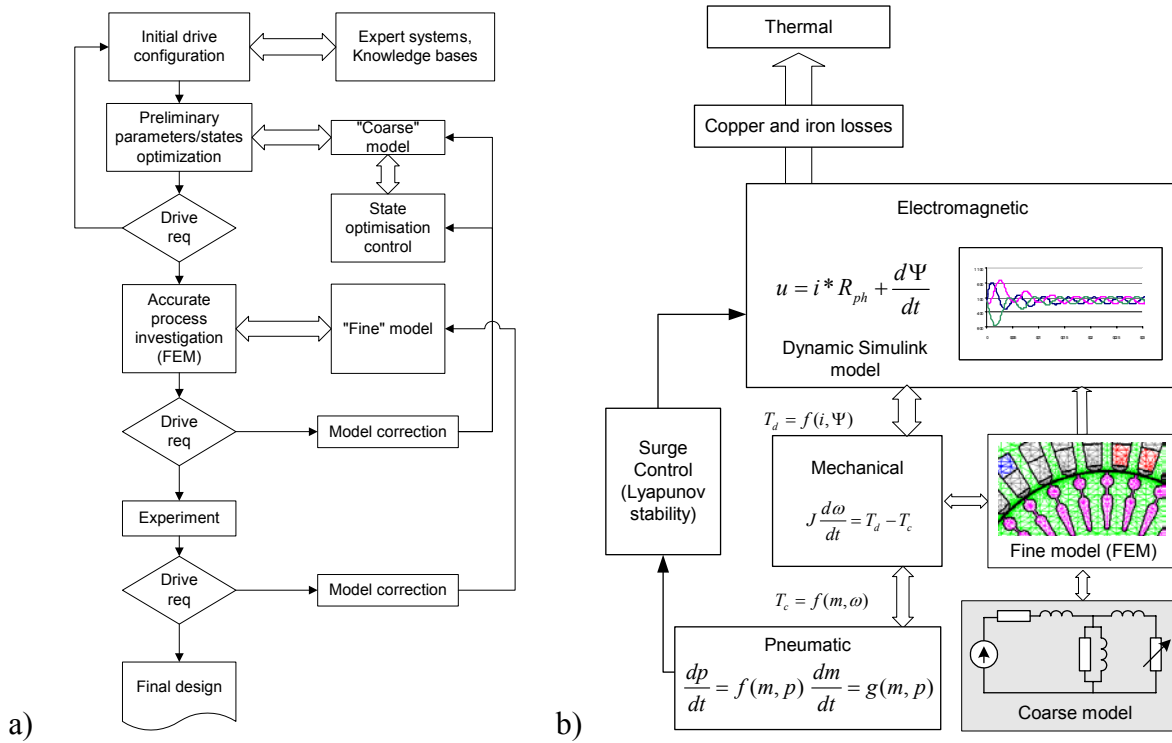


Fig. 4: a) Electrical drive development process; b) Schematic depiction of the dynamic motor model coupled with the load (compressor) and control system

The preliminary design objectives for the electrical drive configuration can be derived from the load (centrifugal air compressor) specification and predicted operation regimes. The mechanical power

consumed by the compressor can be estimated using the following formula [2]:

$$P_c = \frac{c_p T_{01} m}{\eta_c} \left[\left(\frac{P_2}{P_{01}} \right)^{\frac{\gamma-1}{\gamma}} - 1 \right]$$

where η_c – isentropic compressor efficiency.

The compressor performance map is usually supplied by the compressor manufacturer or can be obtained experimentally. In the present study, the initial data for the input power calculation is taken from the map of the “Vortron” compressor. Such type of compressors is designed for the use as a turbocharger in a sport car combustion engine. The rated rotation speed lies in the range of 10000 – 12000 rpm, and it is equipped with an internal gearbox with the ratio of 1/3.45. The compressor performance map and calculated input compressor power are combined in the data sheet (Fig. 5). The compressor operation points, associated with mass flow and pressure are evaluated using the electrochemical equations of the fuel cell and reported in [8].

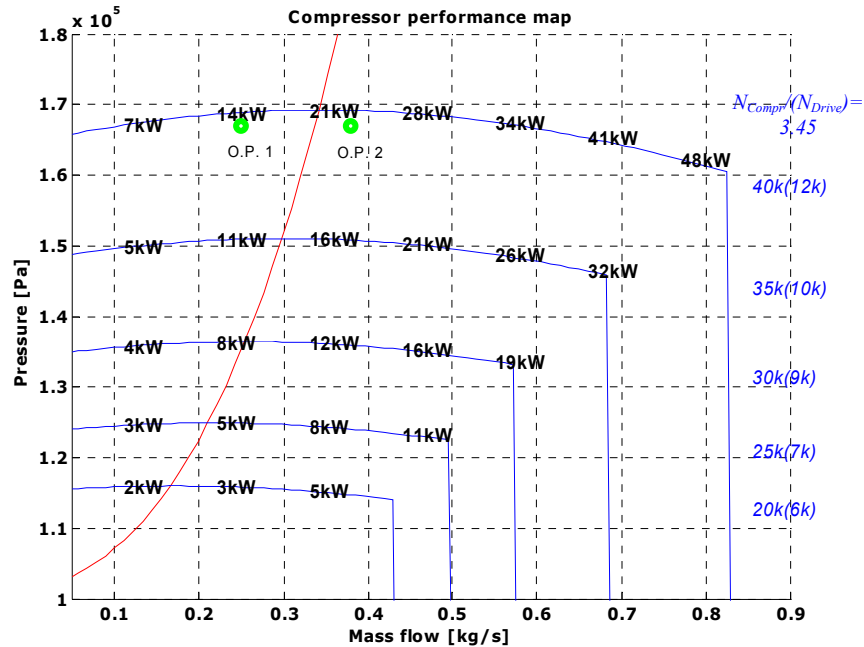


Fig. 5: Compressor performance map with operation points

The high-speed induction motor (IM) is chosen as the compressor drive (direct drive) for the full-scale laboratory experiment. The motor prototype close to the needs of the fuel cell power system compressor has been considered as a benchmark. Its design parameters are specified in Table II.

Table II: Design data of the high speed 2-pole IM

Output power [kW]	30
Terminal voltage line-to-line [V]	500
Frequency [Hz]	300
Phase current [A]	47
Over-current ratio I_a/I_n	6.88
Rated speed [rpm]	17640
Cos (phi)	0.82
Motor efficiency [%]	89.9
Rotor diameter [mm]	110
Stator diameter [mm]	200
Shaft diameter [mm]	50
Air gap [mm]	0.5
Number of stator slots	36
Number of rotor slots	30
Skew width	0.8
Core length [mm]	120

3.1. Coarse model

At the first stage, the electrical machine configuration, defined by system requirements, is analyzed by means of the “coarse” model. The initial induction machine model construction and preliminary design calculation are performed using the design assistant module RMxpert (Rotational Machine Expert) of

Ansoft Co. Maxwell package. The geometric data, winding and bar arrangement, material properties, and main design parameters of the motor are entered as an input of RMxprt. The program input interface panel with general design data of the machine is shown in Fig. 6.

The screenshot shows the 'General' tab of the Maxwell RMxprt software interface. The input fields are as follows:

Parameter	Value
Rated Output Power (kW):	30
Rated Voltage (V):	500
Number of Poles:	2
Frequency (Hz):	300
Rated Speed (rpm):	17640
Stray Loss (W):	740
Friction Loss (W):	700
Iron Core Length (mm):	120
Stacking Factor:	0.95
Steel Type:	D23
Operating Temperature:	75

Winding Connection: Wye Delta

Load Type:

A small graph titled 'Fan Load' is visible, showing a curve that rises to a peak and then falls.

Fig. 6: General motor data

The performed calculations are based on the combined analytical and magnetic equivalent circuit design methods which allow the evaluation of a complicated system with the help of a simplified mathematical model by means of lumped parameters. Therefore, it is relatively easy to implement and provide the desired computational efficiency during the design process but it has not a high accuracy level.

The post processor performs the following tasks: display the laminations and winding arrangement, display the design output data parameters, plot the solutions as a set of curves, complete a customized design sheet, view the parametric solutions, convert the model for further finite element analysis and create a Maxwell 2D FEM Project. As an output example, the performance characteristics for the rated regime are shown in Fig. 7.

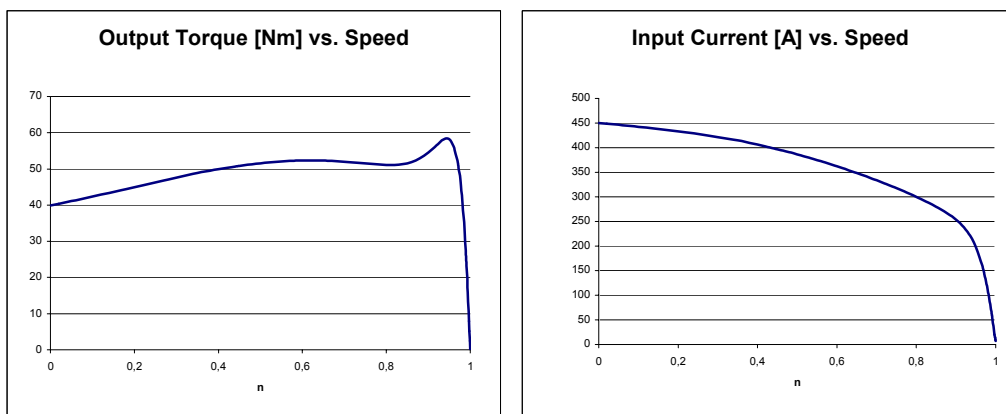


Fig. 7: Obtained performance curves of the IM at rated voltage

3.2. Fine model

For further motor investigation and its performance prediction including the transient electromagnetic process associated with rotational movement, the detailed (fine) electromechanical model of the induction motor is implemented in the Maxwell 2D transient solver. This software module provides the possibility to solve coupled motion, circuit and field equations in time-domain using the finite element method (FEM).

In general, the electromagnetic problem with involved motion is described by the following time-dependent magnetic diffusion equation [9]: $\frac{1}{\mu} \nabla \times \nabla \times A = J_s - \sigma \frac{\partial A}{\partial t} - \sigma \nabla V + \nabla \times H_c + \sigma v \times \nabla \times A$, where A – magnetic vector potential; V – electric scalar potential; J_s – current source density; H_c – coercivity; v – velocity of moving parts, σ – conductivity, μ – permeability .

The above equation is simplified in such a way, that only a two dimensional problem is investigated and there are no permanent magnets introducing H_c . The further simplification is achieved using the approach, when the reference frame is fixed with respect to the investigated components, thus eliminating the component containing the relative velocity. Finally, the above equation is reduced up to the following:

$$\frac{1}{\mu} \nabla \times \nabla \times A = J_s - \sigma \frac{dA}{dt} - \frac{\sigma}{l} V_b, \text{ where } l \text{ – machine depth; } V_b \text{ – voltage difference across a conductor.}$$

The stator circuit equations with stranded conductors are derived applying Kirchhoff's law and represented in the following form: $d_f \frac{N_f l}{S_f a} \iint \frac{dA}{dt} dS_w + R i_f + L \frac{d i_f}{dt} + u_c = u_s$, where u_s – terminal voltage; i_f – terminal current; N_f – total conductor number in the winding; a – number of parallel branches in the winding, d_f – polarity; S_f – cross-section area of the coil group; R – equivalent resistance, L – equivalent inductance; u_c – voltage drop across a capacitor, S_w – winding cross-section [10].

In order to avoid integration due to the inclusion of capacitance, it is necessary to introduce another differential equation to relate the capacitor voltage u_c to the current i_f [10]: $i_f - C \frac{d u_c}{dt} = 0$.

For the squirrel cage rotor the solid conductor circuit equations are applied:

$r_e \{i_b\} + l_e \left\{ \frac{d i_b}{dt} \right\} = -[M][M]^T \{V_b\}$ and $\{J_b\} = -\sigma \left\{ \frac{dA}{dt} \right\} + \frac{\sigma}{l} \{V_b\}$, where r_e and l_e – the end ring resistance and inductance, $[M]$ connection bar matrix, i_b and J_b - bar current and current density respectively, V_b – bar voltage.

The motion equation is the following: $J \frac{d\omega}{dt} = T_{em} - T_{load} - K_D \omega$, where J – rotor and load inertia; K_D – damping coefficient, T_{em} – electromagnetic torque, T_{load} – load torque.

The electromagnetic torque is computed employing the method of virtual work. The load torque is equal to the compressor torque in the current system. For simplification, the compressor torque is approximated by a square function of the rotational speed.

The motion of the rotor is introduced by means of independent meshing of two parts of the motor – stationary (stator with slots and windings) and movable (rotor with bars and a shaft) and coupling of them

at the interface. Such a technique allows to avoid remeshing during the mesh movement. The portion of the mesh with the moving surface is shown in Fig. 8.

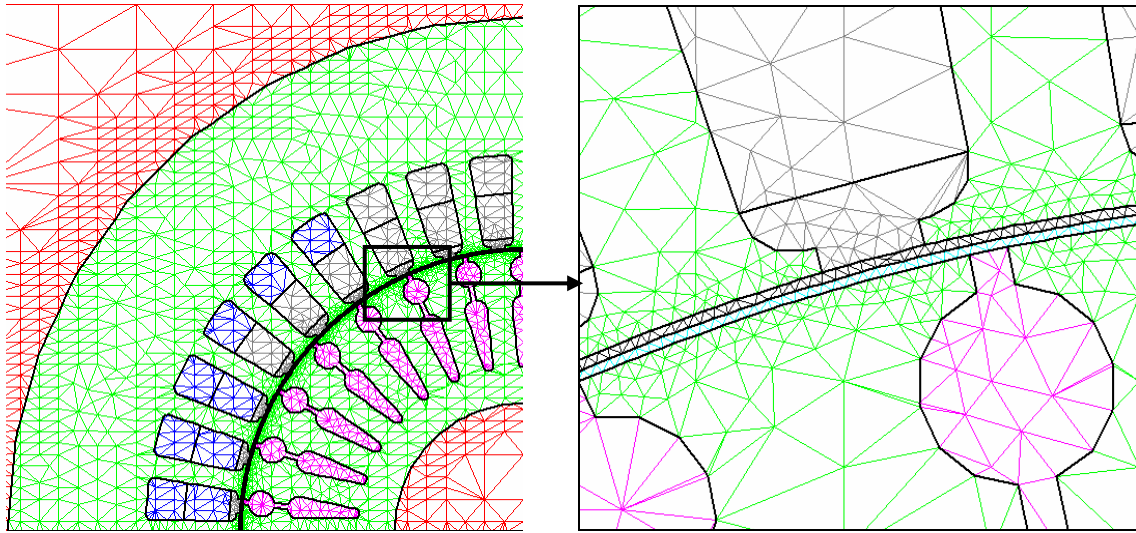


Fig. 8: Fragment of the finite element mesh

4. Simulation results

First, the simulations are performed for the rated operation conditions with the fan type of load. The magnetic flux density distribution over the machine geometry is shown in Fig. 9. The maximum B (around 2 T) occurs in the steel bridges over the rotor bars. The average value of the flux density B in the air gap

is computed using the embedded calculator application by the formula: $B(avg) = \frac{\int Bdl}{\int dl}$ and equals 0.37 T.

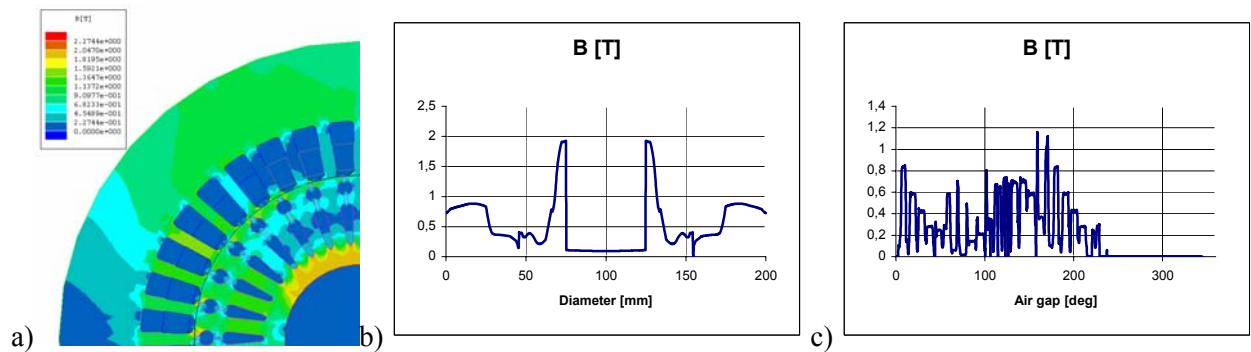


Fig. 9: Field (flux density) distribution; a) all surfaces, b) vertical diameter, c) air gap

The dynamic simulations of the induction motor are performed for two operational points (o.p.1 and o.p.2), defined on the compressor map (Fig. 5). To avoid long time calculation related to the mechanical transient, the initial condition for the rotational speed is set to a value close to the synchronous one. At the time instant of 0.1s the load torque is gradually increased, that imitates the changing of the position of a back-pressure valve. The simulated responses of rotational speed and electromagnetic torque are presented in Fig. 10. The observed torque pulsations (Fig. 10b) in the machine occur due to the stator and rotor slots'

relative movement and the rotor position alignment with respect to the stator winding. The simulations are performed on the CPU AMD 1400 MHz, 512 MB RAM and take approximately 10 hours.

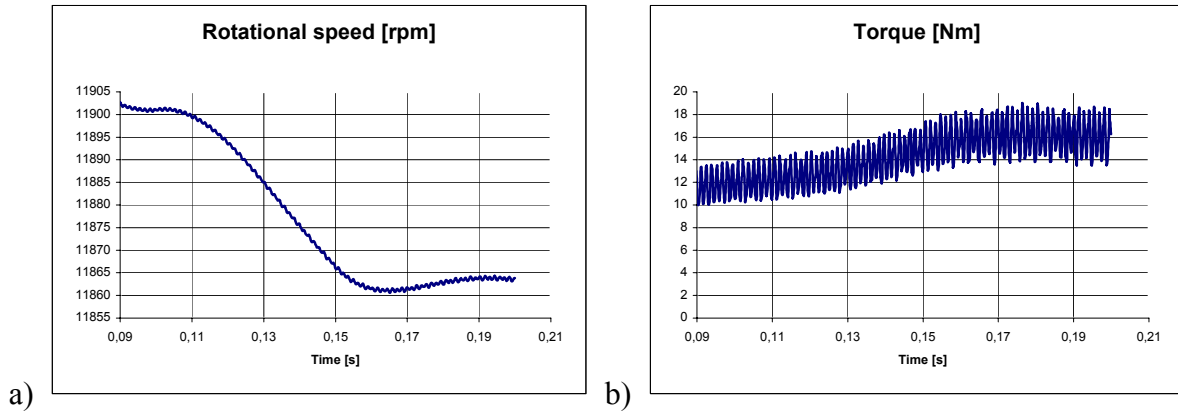


Fig. 10: Transient simulation results; a) Rotational speed, b) Electromagnetic torque

5. Conclusions

The paper presents the intermediate stage of the compressor drive development and analysis for the application in a FC power system. The desired system operation points are preliminary defined using the electrochemical equations of fuel cells and the thermodynamic equations of a compressor consequently. The initial design data are processed, and the motor performance curves are obtained using the design assistant software package RMxpert, Ansoft Co. The transient responses of the high-speed induction motor at the specified operation points of the compressor are simulated. The modelling method uses the coupled circuit, field and motion equations, which are solved using the finite element method in Maxwell 2D software package. The described design and modelling approaches are regarded as a basic strategy for further analysis and control development of the electrical drive for fuel cell power systems.

6. References

- [1]. L. Carrette, K. A. Friedrich U. Stimming, "Fuel Cells Fundamentals and Applications", Fuel Cells 2001, 1, No. 1, 2001
- [2]. J. Larminie, A. Dicks, "Fuel Cell Systems Explained", John Wiley & Sons, LTD, 2000.
- [3]. J. M. Cunningham, "Air System Management for Fuel Cell Vehicle Applications", Master Thesis, Virginia Polytechnic Institute, April 30, 2001. University of California, Davis, 2001.
- [4]. J. Kim, S. M. Lee, S. Srinivasan. "Modeling of Proton Exchange Membrane Fuel Cell Performance with an Empirical Equation." J. Electrochem. Soc., Vol. 142, No. 8, Aug. 1995. pp. 2670-2674.
- [5]. J. C. Amphlett, R. M. Baumert, R. F. Mann, B. A. Peppley, P. R. Roberge, "Performance Modeling of the Ballard Mark IV Solid Polymer Fuel Cell", J. Electrochem. Soc., Vol. 142, No. 1, Jan. 1995, pp. 1-15.
- [6]. J. T. Gravdahl, O. Egeland, "Speed and surge control for a low order centrifugal compressor model", Proceedings of the 1997 IEEE International Conference on Control Applications, 1997, pp. 344 -349.
- [7]. J. T Gravdahl, O. Egelan, S. Vatland. "Active surge control of centrifugal compressors using drive torque" Proceedings of the 40th IEEE Conference on Decision and Control, 2001, pp. 1286 -1291.
- [8]. K. O. Boinov, A. J. A.Vandenput, E. A. Lomonova, "Electrical Drives Operation within a Fuel Cell Power System", 2nd IFAC Conference on Mechatronic Systems, 2002, Berkeley, USA, pp. 49-54.
- [9]. P. Zhou, S. Stanton, Z. J. Cendes, "Dynamic modeling of electric machines", www.ansoft.com.
- [10]. Maxwell 2D (Ansoft Co.) on-line help system.